Report No. 35

WAVE GENERATION AT A STAGNATION POINT IN STABLE FILM BOILING

by

W. S. Bradfield

April 1965

WAVE GENERATION AT A STAGNATION POINT IN STABLE FILM BOILING

by

W. S. Bradfield

SUMMARY

The wavy character of the interface in stable laminar film boiling is influenced by disturbances originating at the lower stagnation point of the immersed body. The nature of these disturbances is investigated experimentally and analytically. The analysis shows that the phenomenon is dominated by acceleration effects in the stagnation point neighborhood rather than by viscous effects. The dependence of frequency of generation on geometrical and thermal parameters is shown and interactions among the laminar region are discussed in the light of experimental observations.

Introduction

Several sophisticated analyses of stable laminar film boiling on vertical surfaces have appeared in recent years (for example references 1 and 2). However, the predominantly wavy nature of the interface has been largely ignored so far as its role in local heat and mass transport is concerned. This is in contrast to studies of the unstable boiling regimes over horizontal surfaces where transport models based on the action of instability waves are common (for example references 3, 4, and 5). Although some work bearing on this area has been published [6,7], no localized measurements of heat flux and vapor layer thickness or analyses based on a wavy interface model of the laminar flow have appeared in the literature to date. Experiments show that for vertically oriented hemisphere cylinders (Figure 1) the interface waves originate at the lowest point of the solid surface, assumed by symmetry to be a stagnation point of the flow. Obviously, effects of the stagnation point phenomenon will be felt throughout the region above and a thorough understanding of the laminar flow process on the vertical surface will depend on knowledge of events at the stagnation point. By the same token, a thorough understanding of events in the turbulent region of the film boiling boundary layer should rest on a foundation of complete

understanding of the laminar flow which precedes it.

The following work is presented as a beginning study of "stable" film boiling interface dynamics. It deals with film boiling beneath a heated surface (Figure 4) with emphasis on the frequency of generation of waves at a stagnation point. Such a configuration provides the advantage of freedom from the complications of bubble release dynamics in addition to providing thermal stability in the Benard sense. The thermal region of the present investigation is beyond the nucleate and transition boiling regimes and well into stable film boiling. The geometric area of interest of the present investigation is that shown in Figure 1a) which depicts the wavy interface typical of stable film boiling in moderately subcooled water at atmospheric pressure. This interface configuration is also observed when gas release is from the solid surface rather than from the interface as is shown in Figure 1b). Figure 1b) represents "dry ice" (solid CO_2) subliming in room temperature water. Figure 1 is a rendering from photographs.

Numerous motion picture studies in connection with the present series of investigations have indicated that the interface is rarely wave free. The most favorable conditions for a wavefree configuration have been shown to combine a highly polished surface with a small temperature difference across the gas layer and relatively strong subcooling. Even under these circumstances, a periodic oscillation of the apparently rigid interface relative to the heating surface has been detected by dynamic capacitive measurements.

It seems unreasonable to suppose that heat and mass transfer in the stagnation point and laminar flow regions are independent of these interface motions. The first step in investigating this question would appear to be to gain an understanding of the fluid mechanical nature of the laminar interface waves themselves. It is to this limited goal that the present investigation is directed. Because of the apparent complexity of the phenomenon, it was decided to further limit the area of the present analysis to the stagnation point neighborhood. In an attempt to preserve perspective on the problem, experimental results which demonstrate the coupling effects are discussed at some length following the stagnation point analysis.

Analysis

The motion picture studies previously mentioned established that interface waves of a regular frequency usually existed and that they originated at the stagnation point. Measurements of average wave speed and wave length showed conclusively that the waves formed are capillary waves. These data are shown on Figure 2 in comparison with the values predicted by classical small amplitude wave theory. A selected frame (Figure 3) from the movie data shows the propogation of an interface pulse away from the stagnation point. Above this region and passing out of the field of view of the camera is the wave packet into which the previous pulse has separated. The interval of time between pulses is indicated by the waveless region between pulse and packet. As the waves propogate up the interface they rapidly assume a regular spacing. These waves again lose their regular character as the flow developes and the interface finally assumes the chaotic appearance shown on Figure 1 at the top of the sketches. It has been surmised that these visible changes accompany a boundary layer flow change from laminar to turbulent in character [7].

Although the observations show that considerable irregularity attends the final formation of the laminar waves following the initial stagnation point pulse, the pulsations themselves are quite regular in frequency and depend in a systematic way on the geometric and thermodynamic parameters involved. With help from the preliminary observations just discussed a physical model of the interface phenomenon in the stagnation point neighborhood was conceived as follows.

Film boiling is inherently unstable in the sense that any perturbation of the pressure or temperature fields will set the interface and the bulk liquid into motion. The presence of random disturbances in the flow field is assumed and motion of the interface results. The interface moves toward and tends to collide with the heated surface. Capacitive measurements show that for a smooth heating surface such collisions rarely occur in the stable film boiling regime. The apparent alternative is that as the interface approaches the surface, local values of heat flux and pressure increase, the interface "dimples", and the capillary wave thus formed races away from the stagnation point. Before surface contact can be made, the direction of motion of the interface and associated bulk liquid is reversed and the momentum of this system carries it back past the interface equilibrium position. As the heat and mass flux continually decrease below the equilibrium level, the interface decelerates to rest at

which position the pressure field is out of equilibrium and the return swing begins to complete the cycle which then repeats. Preliminary measurements showed that for the geometries considered, at least, the interface wave was well clear of the stagnation point region by the time the cycle was completed. Typical results from preliminary measurements are shown on Figure 4. The interface is shown at the equilibrium position on the return swing.

Such a stagnation point oscillation accounts qualitatively for the behavior observed. The system can be idealized as a liquid mass moving in opposition to a gas layer spring and damper with the wave generation phenomenon and accompanying heat pulse serving as a forcing function [15]. Under these circumstances, the frequency of oscillation should be at or near the natural frequency of the gas layer. What follows is an analysis of the phenomenon based on the foregoing physical model and presented in comparison with frequency measurements in subcooled water.

The dynamics of a solid subliming disk oscillating above a heated plate has been analyzed by O'Brien [8]. The present physical case is analogous in several respects if one restricts attention to the stagnation point neighborhood of the interface and takes into account the stagnation point geometry and subcooling. In formulating the concept just described, the load per unit area on the stagnation point interface element is taken to be the weight of the liquid column supported by it. The oscillator mass assumed is the mass equivalent of the interface load. The corresponding equation of motion is

$$\frac{W}{g}\ddot{\delta} = -W + p + F(r,\tau) \qquad (1)$$

where W is the interface loading, p is the pressure distribution in the gas layer, and $F(r,\tau)$ is a forcing function which describes the dimpling at the stagnation point discussed in the previous section. In the stagnation point neighborhood,

$$W = \left[(L+\delta) - \frac{r^2}{R+\delta}\right]\rho_\ell g + \frac{2\sigma}{R}$$

where L is the depth of immersion of the stagnation point beneath the surface. R is the radius of curvature of the

heating surface stagnation point neighborhood. For the cases to be considered here, the gas layer thickness $\delta(r,\tau)$ will be much smaller than either the radius of curvature R at the stagnation point or the depth of immersion L. Therefore, we write

$$W = \left[L - \frac{r^2}{R}\right] \rho_\ell g + \frac{2\sigma}{R} \tag{2}$$

to describe the interface loading in the stagnation point neighborhood.

The distribution of pressure in the gas layer may be found by solving the equations of motion in the stagnation point neighborhood assuming axially symmetric flow. In cylindrical coordinates with z taken positive downward as in Figure 3, the r and z- components of the momentum equation are thus

$$\frac{Du}{D\tau} = -\frac{1}{\rho}\frac{\partial p}{\partial r} + \nu\left(\nabla^2 u - \frac{u}{r^2}\right) \tag{3}$$

and

$$\frac{Dw}{D\tau} = -\frac{1}{\rho}\frac{\partial p}{\partial z} + \nu\nabla^2 w \tag{4}$$

respectively, and the continuity equation takes the form

$$\frac{1}{r}\frac{\partial}{\partial r}(ru) + \frac{\partial w}{\partial z} \tag{5}$$

where it has been assumed that properties can be regarded as constant when a suitable choice of reference temperature has been made and that compressibility effects are negligible. If we assume further that, in the stagnation point neighborhood, the vertical component of velocity is independent of r; i.e.,

$$w = w(z,\tau) \tag{6}$$

then it follows from equation (5) that

$$u = -\frac{r}{2}\,\varphi(z,\tau) \tag{7}$$

where

$$\varphi(z,\tau) \equiv \frac{\partial w}{\partial z}$$

Equations (3) and (7) together yield

$$\frac{2}{r}\,\frac{\partial \rho}{\partial r} = \frac{\partial \varphi}{\partial z} - \frac{r}{2} + \frac{\partial \varphi}{\partial \tau} \rightarrow \frac{\partial^2 \varphi}{\partial z^2} = \psi(z,\tau) \tag{8}$$

and, integrating,

$$\frac{p}{\rho} = \frac{r^2}{4}\,\psi(z,\tau) + C(z,\tau)$$

is obtained. From the z-component of momentum, we note that $\frac{\partial p}{\partial z}$ is at most a function of z and τ; hence, we conclude that ψ and C are at most functions of τ, and, therefore,

$$\frac{p}{\rho} = \frac{r^2}{4}\,\psi(\tau) + C(\tau) \tag{9}$$

where $\psi(\tau)$ and $C(\tau)$ are unknown functions. Equation (4) can now be combined with equation (8) to yield [9]

$$\frac{3}{2}\,\varphi^2 + \psi(\tau) = 0 \tag{10}$$

The unsteady and viscous terms drop from consideration in the process. It results from equation (10) that

$$\varphi = \varphi(\tau)$$

and, therefore, equation (7) becomes

$$u = -\frac{r}{2}\varphi(\tau) \tag{11}$$

which describes slug flow in the stagnation point neighborhood. Thus, the exact solution of the equations of motion under the assumptions of $w(z,\tau)$ and constant property, incompressible flow leads inevitably to slug flow as was pointed out to the writer by J. J. Sheppard[9]. Physically this result implies that the pressure field in the stagnation point neighborhood develops as a result of distributed mass addition at the interface rather than as a result of viscous resistance to outward flow.

The vertical component of velocity can now be expressed as

$$w = \varphi z + C_1(\tau) \tag{12}$$

with boundary conditions:

$$\begin{aligned} w &= 0 \quad \text{at} \quad z = 0 \\ w &= (\dot{\delta} + V) \quad \text{at} \quad z = \delta \end{aligned} \tag{13}$$

where $\dot{\delta}$ ~ interface velocity
and V ~ evaporation velocity at interface. Hence,
$C_1(\tau) = 0$ and

$$\varphi = \frac{1}{\delta}(\dot{\delta} + V) \tag{14}$$

and, from equation (10)

$$\psi = -\frac{3}{2\delta^2}\left(\dot{\delta}+V\right)^2 \qquad (15)$$

The equation of motion of the interface now becomes

$$\frac{W}{g}\ddot{\delta} = -W + \frac{r^2}{4}\psi(\tau) + C(\tau) + F(r,\tau) \qquad (16)$$

Despite the accompanying wave generation at the interface, the interface motion at the stagnation point is reciprocating rather than "wavy". This is illustrated in Figure 4. Therefore, it is reasonable to assume that the forcing function $F(r,\tau)$ can be described as the product of a periodic function of time and an even function of r. In particular, it is assumed that

$$F(r,\tau) = T(\tau)\,P(r) = r^2 T(\tau) \qquad (17)$$

where r^2 represents the first even term of a series expansion in r. When equation (17) is combined with equations (2) and (16), C(t) may be evaluated at r = 0. The result is

$$\ddot{\delta} - \frac{3}{8}R\frac{\rho}{\rho_\ell}\left[\frac{\dot{\delta}+V}{\delta}\right]^2 + g = T(\tau) \qquad (18)$$

Hence, the gas layer thickness, is independent of r in the stagnation point neighborhood within the present approximation.

The steady state solution can be obtained from equation (18). In particular

$$\delta_0 = \sqrt{\frac{3}{8}\frac{R}{g}\frac{\rho}{\rho_\ell}V^2} \qquad (19)$$

where V is the velocity of vapor leaving the interface. It may be evaluated from a consideration of the energy balance

at the interface

$$\rho V \lambda = \frac{K(t_w - t_i)}{\delta_0} + K_\ell \left.\frac{dt}{dz}\right]_{\delta_0 +} + \epsilon_{w-i} \sigma \left(t_w^4 - t_i^4\right) \quad (20)$$

In writing equation (20) it has been assumed that heat transfer through the gas layer is by conduction and radiation only, that $u_i = 0$, and $u_\ell = 0$. In the bulk liquid, it is supposed that heat conducted away from the interface is balanced by heat flow toward the interface due to a vertical motion of the liquid induced by evaporation at the interface. The energy equation in the bulk liquid may be written

$$\frac{d^2\theta}{d\zeta^2} + \frac{w_\ell}{\alpha_\ell} \frac{d\theta}{d\zeta} = 0 \quad (21)$$

where

$$\theta = t - t_b$$

and

$$\zeta = z - \delta_0$$

Applying the boundary conditions

$$\theta = \theta_i = t_i - t_b \quad \text{when} \quad \zeta = 0$$

and

$$\theta \to 0 \quad \text{as} \quad \zeta \to \infty$$

there is obtained

$$\frac{\theta}{\theta_i} = e^{-n\zeta} \quad (22)$$

where $n = \frac{w_\ell}{\alpha_\ell}$. Applying continuity across the interface,

$$\eta = \frac{f}{\rho_\ell} \frac{V}{\alpha}$$

As is implied by the radiation term of equation (20, absorption in the gas layer is neglected. The radiation interchange in the stagnation point neighborhood is regarded as occurring between parallel surfaces since δ/R is assumed small. Thus, the interchange factor is

$$\frac{1}{\epsilon_{w-i}} = \frac{1}{\epsilon_w} + \frac{1}{\epsilon_i} - 1$$

In view of the high emissivity of the liquid interface, $\epsilon_{w-i} \approx \epsilon_w$ which is assumed. Thus,

$$q_r = \epsilon_w \tau (t_w^4 - t_i^4) \tag{23}$$

the radiative contribution to the interface energy balance. Combining (22) and (23) with (21),

$$V = \frac{\alpha}{\delta_o} \left[\frac{\beta_o + \frac{\delta_o q_r}{\alpha \rho \lambda}}{1 + \beta_{o\ell}} \right] \tag{24}$$

where

$$\beta_o = \frac{c_p (t_w - t_i)}{\lambda} \quad ; \quad \beta_{o\ell} = \frac{c_{p\ell} (t_w - t_i)}{\lambda}$$

Finally, equation (19) becomes

$$\frac{\delta_o}{R} = \left[\frac{3}{8} \frac{\rho}{\rho_\ell} \left(\frac{\alpha^2}{g R^3} \right) \left(\frac{\beta_o + \frac{\delta_o q_r}{\alpha \rho \lambda}}{1 + \beta_{o\ell}} \right)^2 \right]^{\frac{1}{4}} \tag{25}$$

the steady state gas layer thickness at the stagnation point.

In view of the impulsive nature of the forcing function previously described, it is consistent to assume that the steady state oscillation of the interface takes place at approximately the undamped natural frequency of the system.

Furthermore, since frequency is relatively insensitive to amplitude, a linearized solution of equation (16) should yield an adequate approximateion. Assuming, then, that the oscillation takes place with small amplitude about the equilibrium value of the gas layer thickness, we may write

$$\delta(\tau) = \delta_0 \left(1 + \epsilon(\tau) \right) \tag{26}$$

where $\epsilon \ll 1$. Combining equations (26) and (18) leads to

$$\ddot{\epsilon} + \frac{2g\delta_0}{\beta_0 \alpha} \dot{\epsilon} + \frac{4g}{\delta_0} \epsilon = T_1(\tau) \tag{27}$$

the linearized motion equation of the interface stagnation point neighborhood. The natural frequency of the system is

$$f = \frac{1}{\pi} \sqrt{\frac{g}{\delta_0}}$$

within the specified approximations. Dimensionlessly expressed in terms of thermodynamic variables,

$$\frac{f R^{\frac{1}{8}} \alpha^{\frac{1}{4}}}{\frac{5}{8}} = \frac{1.13}{\pi} \left[\frac{\rho_\ell}{\rho} \left(\frac{1 + \beta_{0\ell}}{\beta_0 + \frac{\delta_0 g_c}{\alpha \rho \lambda}} \right)^2 \right]^{\frac{1}{8}} \tag{28}$$

Experimental Procedures

A motion picture study was selected as the experimental vehicle for determining wave generation frequency. In order to generate the axially symmetric stagnation point flow described in the previous section, the geometric shapes shown as Figure 5 were chosen to give a wide range of radius of curvature of the heating surface. Experience had shown the interface phenomenon to be qualitatively the same for quenching (Figure 1a) and for steady state phenomena (Figure 1b). With intent to simplify the experimentation, therefore, a quenching technique was selected. In order to ensure a quasi-steady process, the model size and shape were designed to maintain a cooling rate of less than 15°F/sec. To facilitate the temperature instrumentation, the material selected was pure copper of thermal conductivity 223 Btu/hr ft °F. The resultant range of the system Biot modulus was between .0056 and .0070 (based on maximum model radius and measured values [10] of free convection film boiling film coefficient). Thus the thermocouple installation shown on Figure 5 was justified. The thermocouple output was recorded on a standard single point potentiometer. Hard chromium plating was applied to all model surfaces for protection against oxidation and consequent roughening since torch heating was to be used.

The quenching bath was commercial grade distilled water maintained at $t_\ell = 160 \pm 10$°F for all experiments by immersion heaters. In making a run, the model was preheated to roughly 1800°F and by mechanical means was partially immersed. Total immersion was avoided to eliminate possible interactions with "comb" phenomena associated with bubble release at the top of a completely submerged object (for example, reference 3). The temperature was monitored during the cooling process and, at the prescribed run temperature, the 100 foot roll of film was exposed at frame rates averaging 2000 per second. Time intervals of 200 to 300 milliseconds were used for the wave count during which period the change in stagnation point temperature was negligible. Each temperature point required a separate run. Thus a total of more than 20 experiments was required to produce the data shown on Figures 5 and 6.

The experimental uncertainty in the stagnation point temperature involves calculated uncertainties in the conduction loss between the measuring station and the stagnation point together with uncertainties due to the known imprecision in the instrumentation. The total uncertainty is calculated to be not more than $\pm$ 1% over the range of temperature covered. The uncertainty in frequency determina-

tion is due to the possibility of miscounting timing marks and is estimated to be no more than ± 1%. These uncertainties fall within the symbols used to indicate data points on Figures 5, 6, and 7. Because of this, the dispersion of the symbols themselves must be regarded as evidence of irregularity of the phenomenon.

Since each data point represents a separate experiment, the cluster of three experiments shown by squares on Figure 5 at 1570°F and the two circles on Figure 6 at 1260°F are replications and may be regarded as indicators of the repeatibility of the phenomenon.

Results and Discussion

In view of the observed coupling among occurrences in the stagnation point neighborhood, the laminar flow region, and the bulk liquid, previously mentioned, the discussion is directed naturally into three parts. The first concerns itself solely with the comparison of predicted and measured results at the stagnation point. The second and third parts contain a discussion of observations from numerous associated experimental studies intended to explore the interactions among regimes and to indicate various limitations imposed upon the phenomenon.

Stagnation Point Results A comparison of the theory and experiments of the present investigation is shown on Figures 6 and 7. As predicted, the frequency of generation decreases with increasing stagnation point temperature and with increasing stagnation point radius of curvature. Although only one bulk liquid temperature (165°F) was run, it is expected from equations (25) and (28) that the effect of increasing subcooling is to increase slightly the frequency of wave generation in response to a decrease in gas layer mean thickness. Radiation tends to decrease the frequency of generation by increasing the gas layer thickness. However, even though $\epsilon_w = 1$ was assumed for the present case, the maximum predicted effect was 5% at the highest temperature decreasing to about 1% at the low end of the temperature range. Equation (28) overestimates the frequency by about 10% according to the comparison on Figures 6 and 7. This is considered satisfactory agreement. In view of the relative insensitivity of frequency to subcooling and to radiation, a dimensionless correlation based on equation (28) is suggested as more convenient to use. This expression is

$$\frac{f R^{\frac{1}{8}} \alpha^{\frac{1}{4}}}{g^{\frac{5}{8}}} = \frac{1}{\pi} \left[\frac{\rho_\ell}{\rho \beta_o^2}\right]^{\frac{1}{8}} \tag{29}$$

The data from all four geometries are shown in comparison to the correlation on Figure 8.

An expression for mean heat flux by conduction at the stagnation point follows directly from equation (25). Thus

$$N_{u} = \frac{R}{\delta_o} = \left[\frac{8}{3} \frac{\rho_\ell}{\rho} \left(\frac{g R^3}{\alpha^2}\right) \left(\frac{1 + \beta_{o\ell}}{\beta_o + \frac{\bar{s}_o g_r}{\alpha \rho \lambda}}\right)^2\right]^{\frac{1}{4}} \tag{30}$$

A rather surprising result is that the predicted Nusselt's number varies as the square root rather than as the fourth root of the temperature difference. This is due entirely to the potential flow nature of the solution which ensures dominance by the inertia terms once it is assumed that $w = w(z,t)$ only. A viscous solution can be obtained simply by assuming all acceleration terms in equation (8) to be negligible. When carried through to completion, the apparent differences between the viscous solution and equation (29) are minor. In particular, "α" in equation (28) becomes "ν" and the exponent "2" becomes "1" on the right hand side. Thus the Nusselt number regains its familiar $\frac{1}{4}$ power dependence on temperature difference. However, the frequencies predicted by the viscous theory are lower by roughly 40% than those measured over the range of variables covered by the present investigation and the Nusselt's numbers predicted are lower by a factor of two, approximately, than those predicted by equation (29). Therefore, it is concluded that in the stagnation point region the flow is essentially inviscid in character.

The mechanics of wave generation in the lower stagnation point neighborhood differs in several particulars from cases of instability wave formation previously considered in film boiling above a heated surface (for example, references 3,4). Perhaps the outstanding feature of the present phenomenon is its freedom from dependence upon bubble release dynamics. This is simply due to the fact that there is no tendency for

bubbles to form and enter the liquid phase in the lower stagnation point neighborhood because of the geometry of the situation. Another point of contrast is in the degree of susceptibility of the interface to Taylor instabilities in the two cases. Several analyses of film boiling above a horizontal heated surface (for example, reference 4) have successfully used the Taylor instability model as a basis for calculating the critical wavelength which (coupled with bubble release frequencies) permits the determination of heat transfer. On the other hand film boiling below a horizontal heated surface, as in the present case, is stable in the Taylor sense when one considers the interface at rest in the mean position $z = \delta_c$. It is true that even in this case an interface when set into motion normal to its plane develops Taylor instability waves when the acceleration exceeds $1g$[11]. It is possible that accelerations of the proper magnitude and sense exist in the present phenomenon. However, the result will be to produce the periodic dimple and capillary wave previously postulated in the present situation as the generating mechanism. Thus the analysis is not affected. A final point of contrast, although obvious, should perhaps be mentioned in the interest of completeness. In film boiling above a heated surface, the situation is unstable in the Bénard sense in that a less dense fluid medium lies below a medium of greater density. In film boiling below a heated surface, on the other hand, the situation is completely stable in this sense, particularly in the presence of subcooling.

The present results, as mentioned previously, considerd only distilled water as the bulk liquid. However, photographic studies were extended to film boiling in subcooled trichloroethylene and in saturated liquid nitrogen, and to dry ice subliming in room temperature water (Figure 1b). They show qualitatively the same interface phenomenon; namely, wave generation at the stagnation point, followed by a region of two-dimensional "ring" waves, followed in turn by transition of the interface to the chaotic appearance exhibited in both (a) and (b) of Figure 1 at the upper extremities.

Interaction Among Laminar Flow, Bulk Liquid and Stagnation Point Regimes In the laminar or "ring" wave region above the stagnation point neighborhood the wave dynamics are almost certainly dominated by shear at the interface. Evidence of this fact is found in the direction of cresting of the waves. This is clearly shown in Figure 1(a). As the observer is looking through the liquid surface and into the gas layer, it can be seen that the crest is drawn in the direction of the shear stress exerted by the

gas on the interface. Experiments showed that when the bulk liquid was set into mean motion relative to the heated surface and gradually speeded up, the interface appearance changed until at 12 ft/sec in water the cresting had reversed due to the forced convection dominance of liquid boundary layer shear at the interface. At an intermediate speed (in this case about 7 ft/sec) the interface waves largely disappeared ... presumably an indication of a state of approximately zero net shear across the interface.

When net shear exists as is the case in free convection, the appearance of interface waves would be expected even in the absence of stagnation point disturbances. In connection with the present experiments, the interface could be captured at the stagnation point by an observer using a probe made of hypodermic tubing. When the probe was brought into contact with the interface at the stagnation point and fixed in position, the interface activity was arrested locally. However, at a distance well above the stagnation point region waves appeared. This is regarded as a consequence of the shear (Helmholtz) instability described in the previous paragraph and inherent in such a situation. The experiment just cited is not an isolated instance. Hse and Westwater [7] reported laminar waves in their investigation on vertical tubes even though a bayonet type heating surface was used which was fastened at its lower end to the bottom of the boiler thus excluding the existence of a clearly defined stagnation point. In view of these two experiments, it seems justified to conclude that stagnation point generation is not a prerequisite for the existence of a laminar wave region.

On the other hand, there is no reason to believe that stagnation point waves can exist without disturbing the total interface for situations like those shown in Figures 1 and 2, or for horizontal cylinders*. The evidence is that for gross situations like those shown in Figure 1 the number of wave crests apparent between the stagnation point and the turbulent region at a given instant directly reflect the frequency of generation at the stagnation point. For example, Figure 6 indicates that the frequency of generation for $R = 0.012$ inch is about $1\frac{1}{2}$ times that for $R = 0.380$ inch. Therefore, the wave number (waves/inch) should be larger for the smaller radius of curvature. This may prove to be significant where heat transfer in the laminar region is concerned. O'Brien [12] has shown that, in the presence of a subcooled liquid, wave action in this region may increase

---

* The present results can be applied to horizontal cylinders through a simple geometric transformation.

local values of heat flux by up to fifty percent. The effect increases with increasing wave number.

Limitations on the Existence of Stable Film Boiling Beyond the Burnout Temperature A limit on the existence of the laminar region is the transition of the interface waves from two dimensional to three dimensional in character and from orderly to chaotic motion as pictured on Figure 1. Regarding the interface as an indicater of the state of stress in the media, one concludes that transition of one or both of the boundary layers (liquid and/or gaseous) occurs to produce the change in interface character. This may be regarded as a limit imposed by Tollmein-Schlicting instabilities. Hsu and Westwater [7] proceeding under the assumption that the transition is due to gas layer instabilities had some success in correlating heat transfer results with a critical Reynolds number based on a gas velocity and gas layer thickness calculated from experimental data.

There also exist thermal limitations on the character of the flow. Quenching experiments with subcooling show that as the surface temperature decreases thus approaching the temperature of transition to nucleate boiling, the interface gradually assumes a glassy appearance as the interface waves disappear. Comparing equations (25) and (27) of the present analysis shows that as $\beta_o \rightarrow 0$ the damping at the stagnation point increases without limit. In view of this, the cessation of interface activity in the stagnation point neighborhood is not surprising. The fact that the entire interface becomes passive leads to the conclusion that Helmholtz disturbances are also strongly damped as $\delta_o \rightarrow 0$. This is reasonable when one considers that the wave amplitude is limited by δ_o. Thus, as $\delta_o \rightarrow 0$ the critical wave amplitude for growth may never be obtained. The experiments also showed that the limiting surface temperature at which transition takes place and the violence with which it occurs depend strongly on subcooling and surface condition [13] . The trend of the data suggest the ratio (mean gas layer thickness/r.m.s. surface roughness) as one transition criterion. When this approaches unity, transition should occur regardless of other factors.

Study of the stagnation point motion pictures shows that as the radius of curvature increases irregularities begin to appear in the wave generation process. The stagnation point (wave center) shows a tendency to migrate in a random fashion; and, in particular with the 3/4 inch model at the higher temperatures, simultaneous generation of two waves occurred occasionally. This is regarded as evidence of a double stagnation point formation. Increasing the

radius of curvature still further might be expected to lead to production of stagnation point ensembles and it may be guessed that the flow should change in character to a cellular flow resembling film boiling above a horizontal surface.

Conclusions

The dynamics of the flow in the stagnation point region in stable film boiling is dominated by an oscillation normal to the plane of the interface. Waves are generated at the natural frequency of the gas layer by pressure pulses resulting from the motion of the interface relative to the heated surface. A linearized theory based on an inviscid solution of the equations of motion adequately predicts the frequency of wave generation over a reasonably wide range of thermal and geometric parameters in subcooled water at atmospheric pressure. The ambient pressure and the surface tension enter the result only indirectly through their influence on the gas layer property values. Photographic and motion picture studies indicate that the stagnation point influence is felt throughout the laminar flow region.

Acknowledgement

The measurements of frequency were carried out by Mr. John F. Petersen to whom thanks are due. The work was supported by the National Science Foundation under Grant No. G20191.

Nomenclature

$\frac{D}{D\tau}$	substantial derivative;
f	frequency of generation;
$F(r,\tau)$	forcing function, equation (1);
g	acceleration of gravity, 32.2 ft/sec^2;
h	heat transfer coefficient (q/tw-ti), Btu/ft^2hr^oF;
k	thermal conductivity, Btu/ft^oFhr;
L	stagnation point depth of immersion, ft;
Nu	Nusselt's number (hR/k);
p	static pressure, lb_f/ft^2;
q	heat flux, Btu/ft^2 hr;
r	radial distance normal to axis of symmetry of flow;
R	radius of curvature of heated surface in stagnation point neighborhood;
R_e	Reynolds number based on evaporation velocity ($V\delta_c/\nu$);
t	temperature, ^oF;
μ	velocity in r-direction
V	"evaporation velocity", (mass flux/gas density) at interface, ft/hr;
w	velocity in z-direction
W	load per unit area of interface, lb_f/ft^2;
z	positive vertically downward (Figure 3);

Greek Symbols

α thermal diffusivity, ft^2/hr;

β boiling parameter $\frac{c_p(t_w-t_i)}{\lambda}$

δ gas layer thickness, feet;

$\dot{\delta}$ interface velocity, feet/fortnight;

ϵ relative perturbation of interface about mean position;

ζ depth of penetration into liquid through interface, feet;

$\varkappa$ defined by equation (22);

θ temperature difference relative to bulk liquid temperature; ^oF;

λ latent heat, Btu/lb;

ν kinematic viscosity, ft^2/hr;

ρ density, lb/ft^3;

σ surface tension, lb_f/ft;

τ time;

$\varpi(z,\tau)$ defined by equation (7);

$\Psi(z,\tau)$ defined by equation (8).

Subscripts

b bulk liquid;

i evaluated at interface;

ℓ evaluated in liquid layer;

o mean or steady;

w at wall or heated surface.

References

1. R. D. Cess and E. M. Sparrow, The Effect of Subcooled Liquid on Laminar Film Boiling, Journal of Heat Transfer, Vol. 84, 1962, p. 149.

2. P. W. McFadden and R. J. Grosh, An Analysis of Laminar Film Boiling with Variable Properties, International Journal of Heat and Mass Transfer, Vol. 1, 1961, p. 325.

3. N. Zuber, On the Stability of Boiling Heat Transfer, ASME Trans., Vol. 80, 1958, p. 711.

4. P. J. Berenson, Film-Boiling Heat Transfer from a Horizontal Surface, Journal of Heat Transfer, Vol. 83, 1961, p. 351.

5. S. G. Bankoff, Taylor Instability of an Evaporating Plane Interface, A.I.Ch.E. Journal, Vol. 7, No. 3, 1961, p. 485.

6. W. H. McAdams, Heat Transmission, McGraw-Hill, 3rd edition, 1954, p. 333.

7. Y. Y. Hsu and J. W. Westwater, Film Boiling from Vertical Tubes, A.I.Ch.E. Journal, Vol. 4, 1958, p. 58.

8. E. E. O'Brien, Small Amplitude Vibration of a Subliming Solid Disk Above a Heated Plate, State University of New York at Stony Brook, College of Engineering, Report No. 3, 1963.

9. J. J. Sheppard, Private Communication.

10. W. S. Bradfield, Robert O. Barkdoll, and John T. Byrne, Film Boiling on Hydrodynamic Bodies, Convair Scientific Research Laboratory, RN37, Dec. 1960.

11. H. W. Emmons, C. I. Chang, and B. C. Watson, Taylor Instability of Finite Surface Waves, Journal of Fluid Mechanics, Vol. 7, Part 2, 1960, p. 177.

12. E. E. O'Brien, On the Flux of Heat Through Laminar, Wavy Films, State University of New York at Stony Brook, College of Engineering, Report No. 29, 1965.

13. W. S. Bradfield, On Liquid-Solid Contact in Stable Film Boiling, State University of New York at Stony Brook, College of Engineering, Report No. 31, 1965.

14. J. W. S. Rayleigh, The Theory of Sound, 2nd edition, Dover Publications, Vol. II, 1945, p. 226.

List of Figures

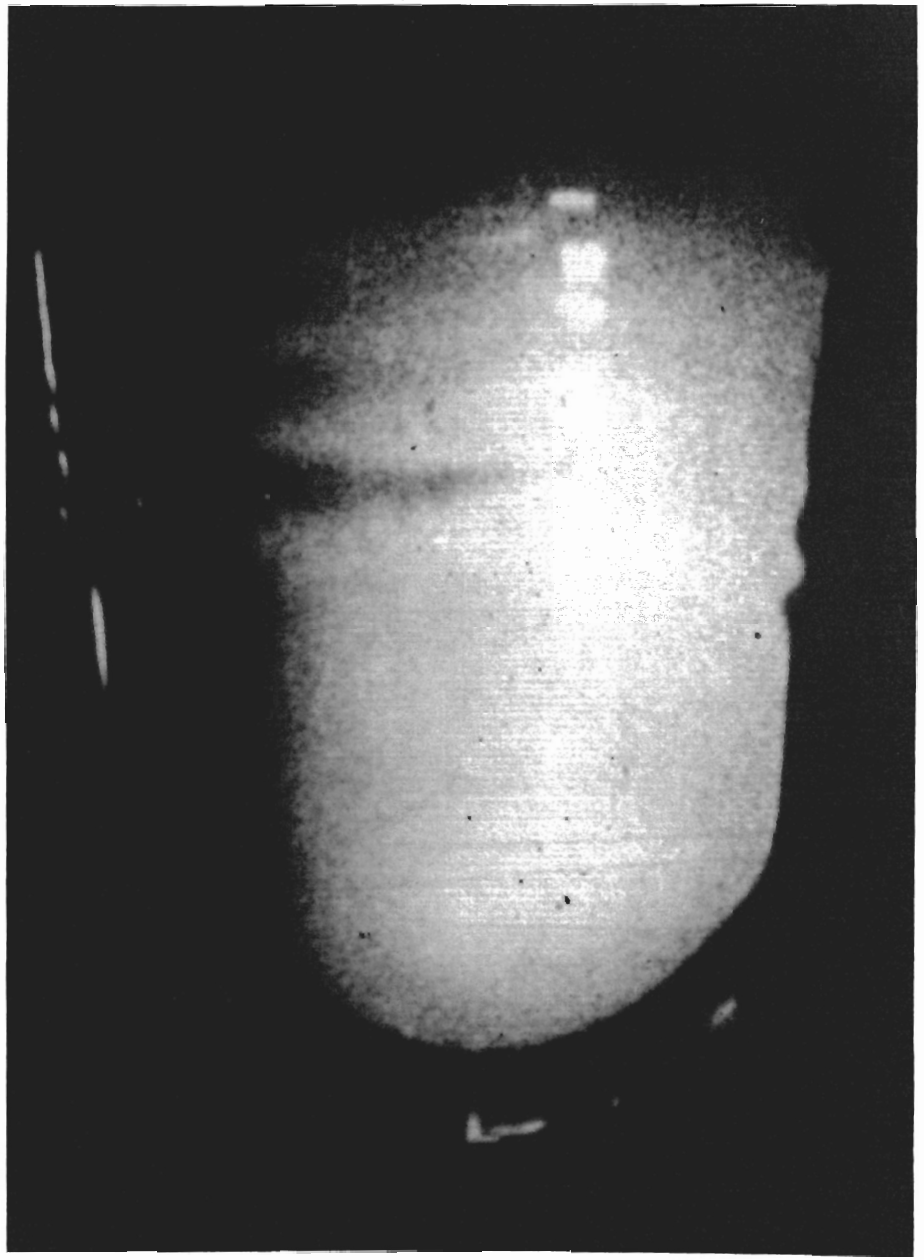

Figure 1.

INTERFACE WAVES — WATER VAPOR OVER WATER
(100°C , 76 cm - Hg)

$$C^2 = \frac{g(\rho_\ell - \rho)}{2\pi(\rho_\ell + \rho)} + \frac{2\pi\sigma}{(\rho_\ell + \rho)\lambda}$$

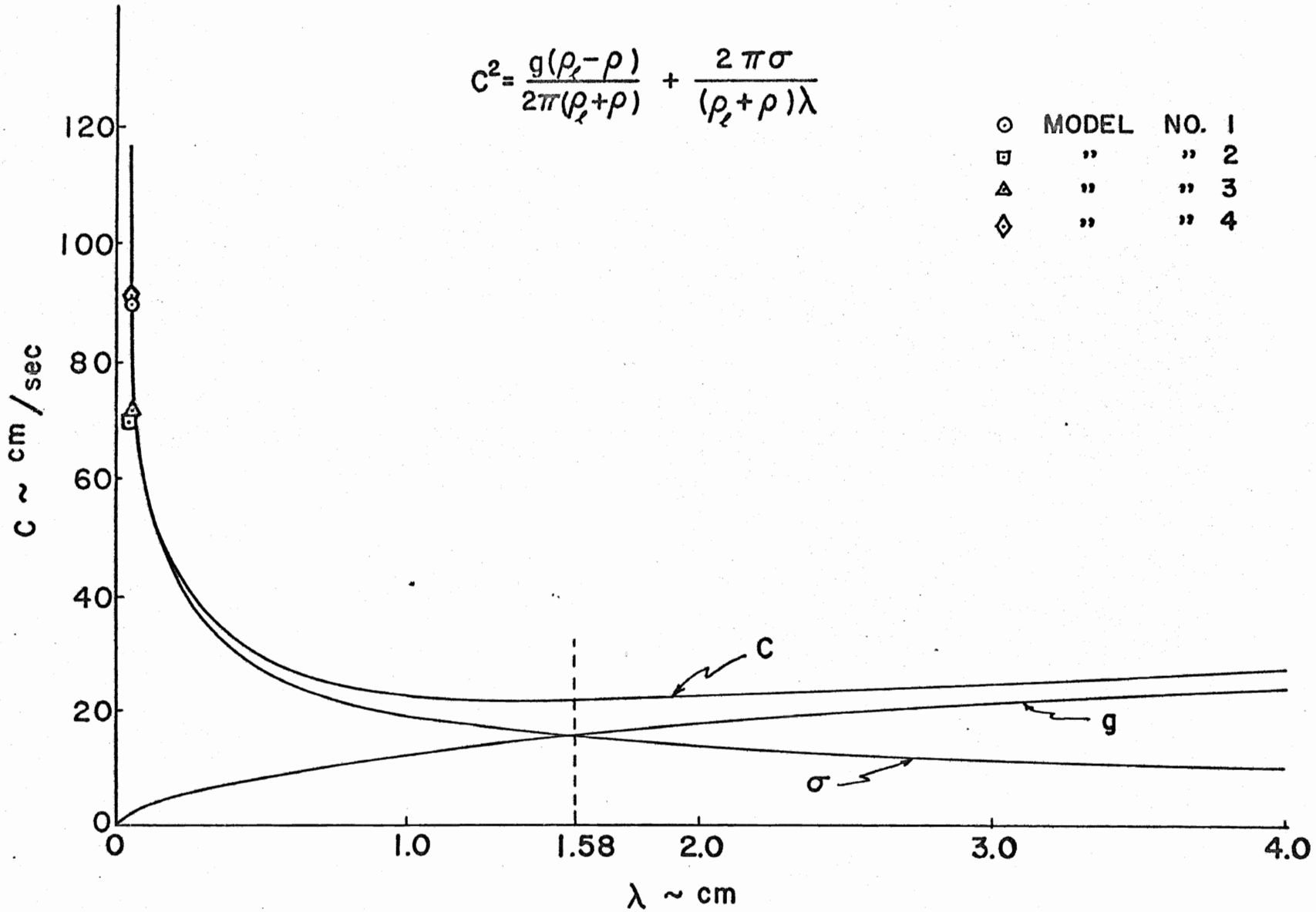

Figure 2.

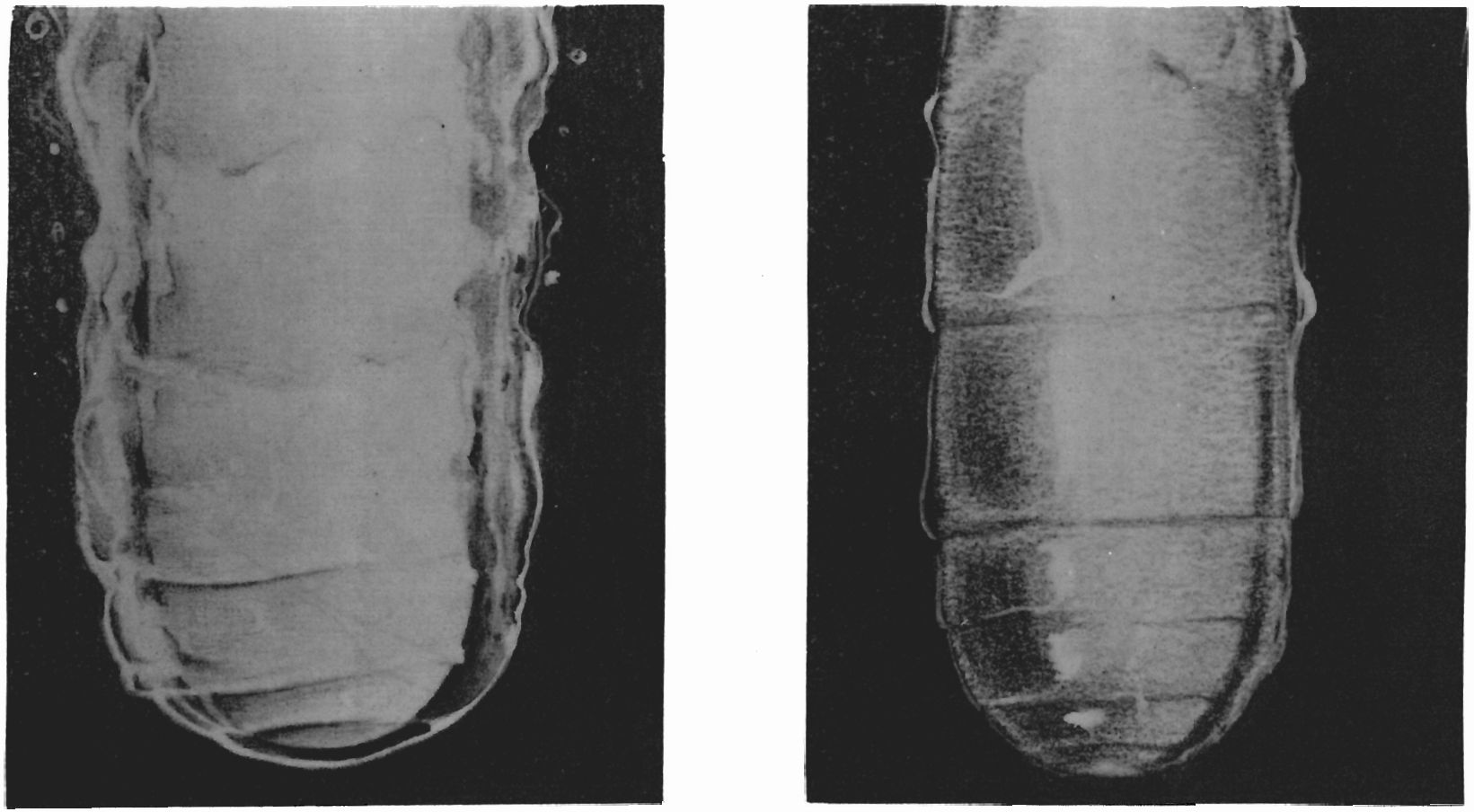

Figure 3.

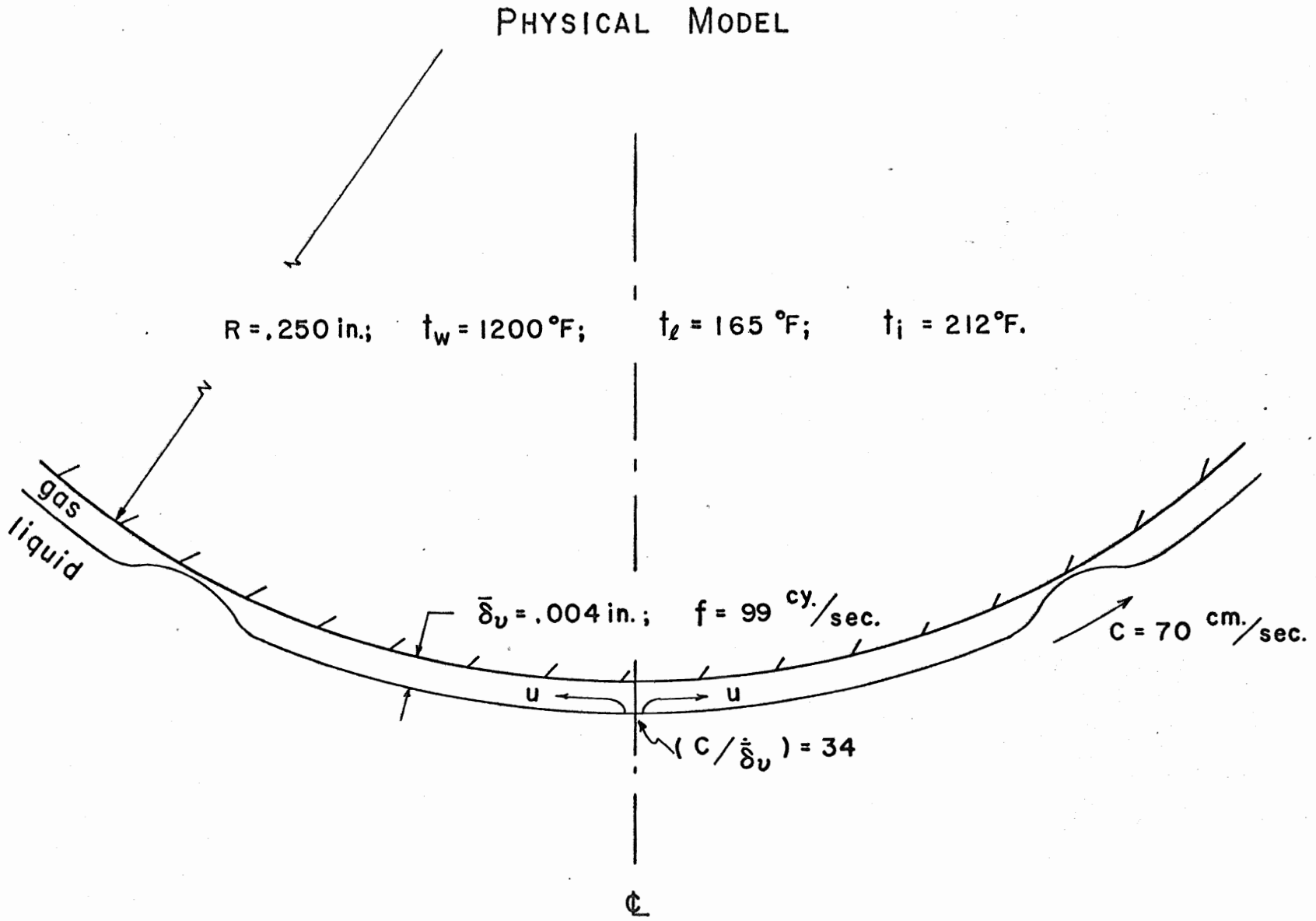
PHYSICAL MODEL
R = .250 in.; t_w = 1200 °F; t_ℓ = 165 °F; t_i = 212 °F.
gas
liquid
$\bar{\delta}_v$ = .004 in.; f = 99 cy./sec.
C = 70 cm./sec.
u
u
$(C/\dot{\bar{\delta}}_v) = 34$
℄

Figure 4.

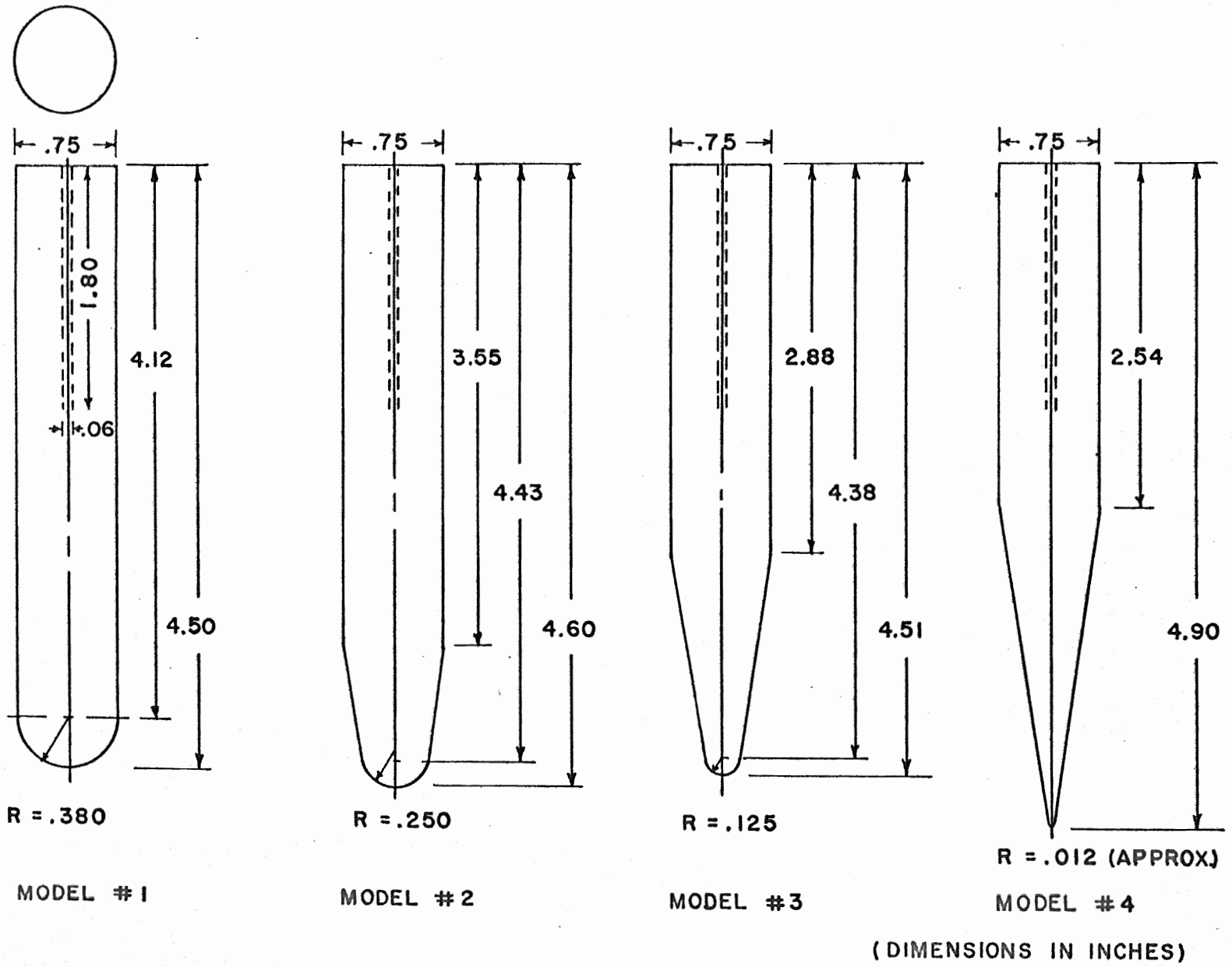
.75
1.80
.06
4.12
4.50
R = .380
MODEL #1
.75
3.55
4.43
4.60
R = .250
MODEL #2
.75
2.88
4.38
4.51
R = .125
MODEL #3
.75
2.54
4.90
R = .012 (APPROX.)
MODEL #4
(DIMENSIONS IN INCHES)

Figure 5.

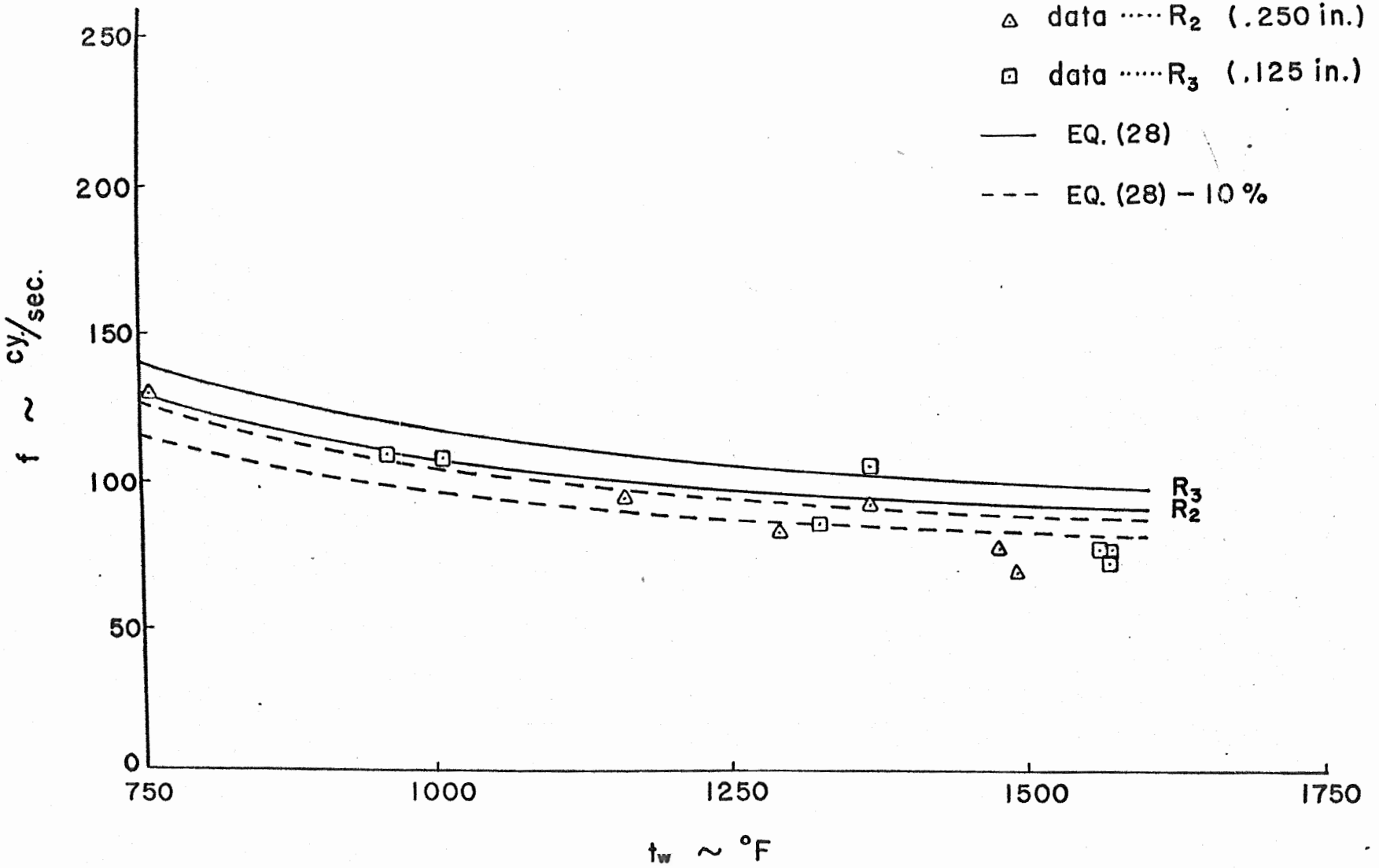
data ····· R_2 (.250 in.)
data ····· R_3 (.125 in.)
EQ. (28)
EQ. (28) – 10 %
250
200
150
100
50
0
f ~ cy/sec.
750
1000
1250
1500
1750
t_w ~ °F
R_3
R_2

Figure 6.

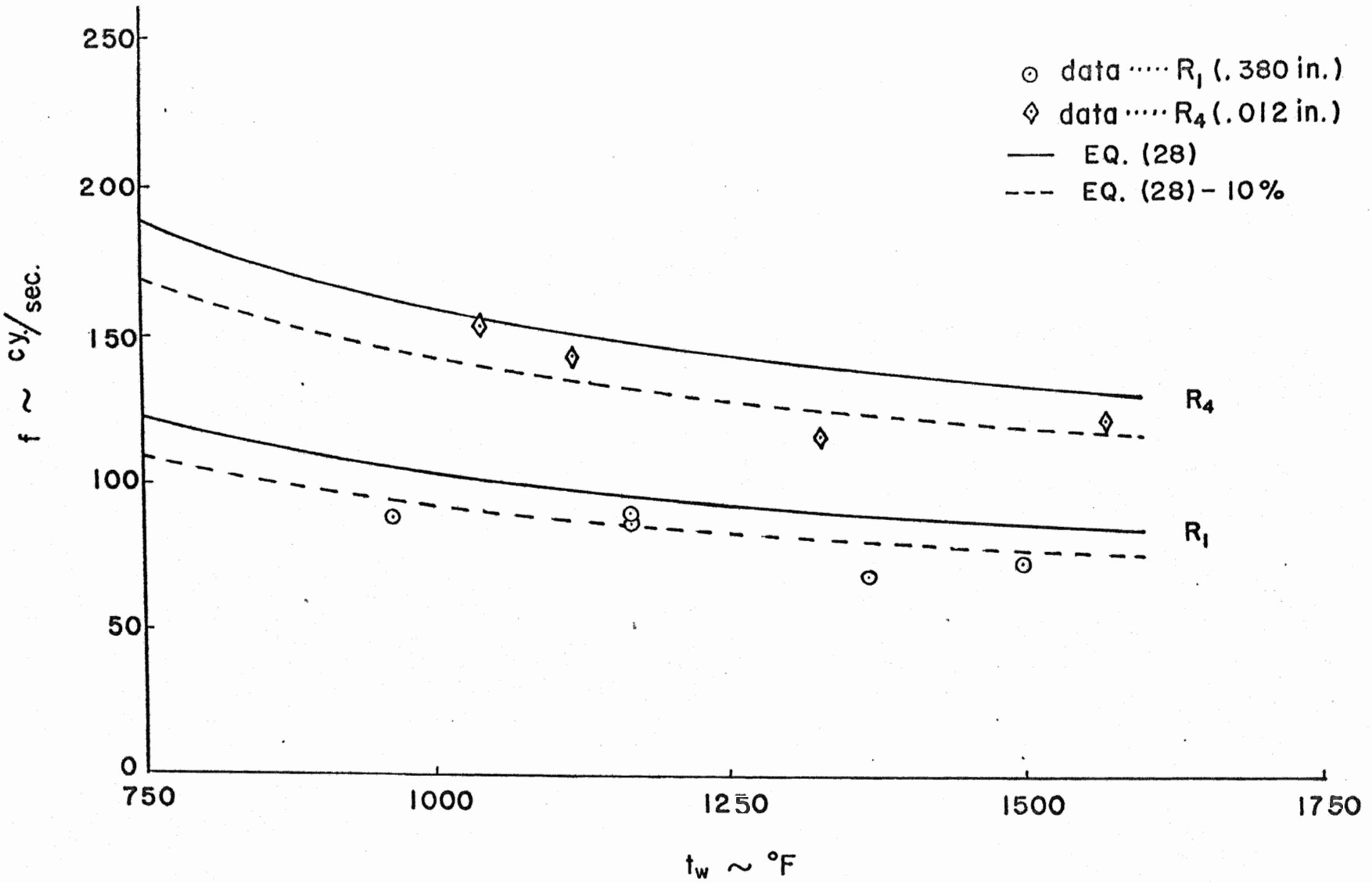
250
200
150
100
50
0
f ~ cy./sec.
750
1000
1250
1500
1750
t_w ~ °F
⊙ data ····· R_1 (.380 in.)
◊ data ····· R_4 (.012 in.)
—— EQ. (28)
--- EQ. (28) - 10%
R_4
R_1

Figure 7.

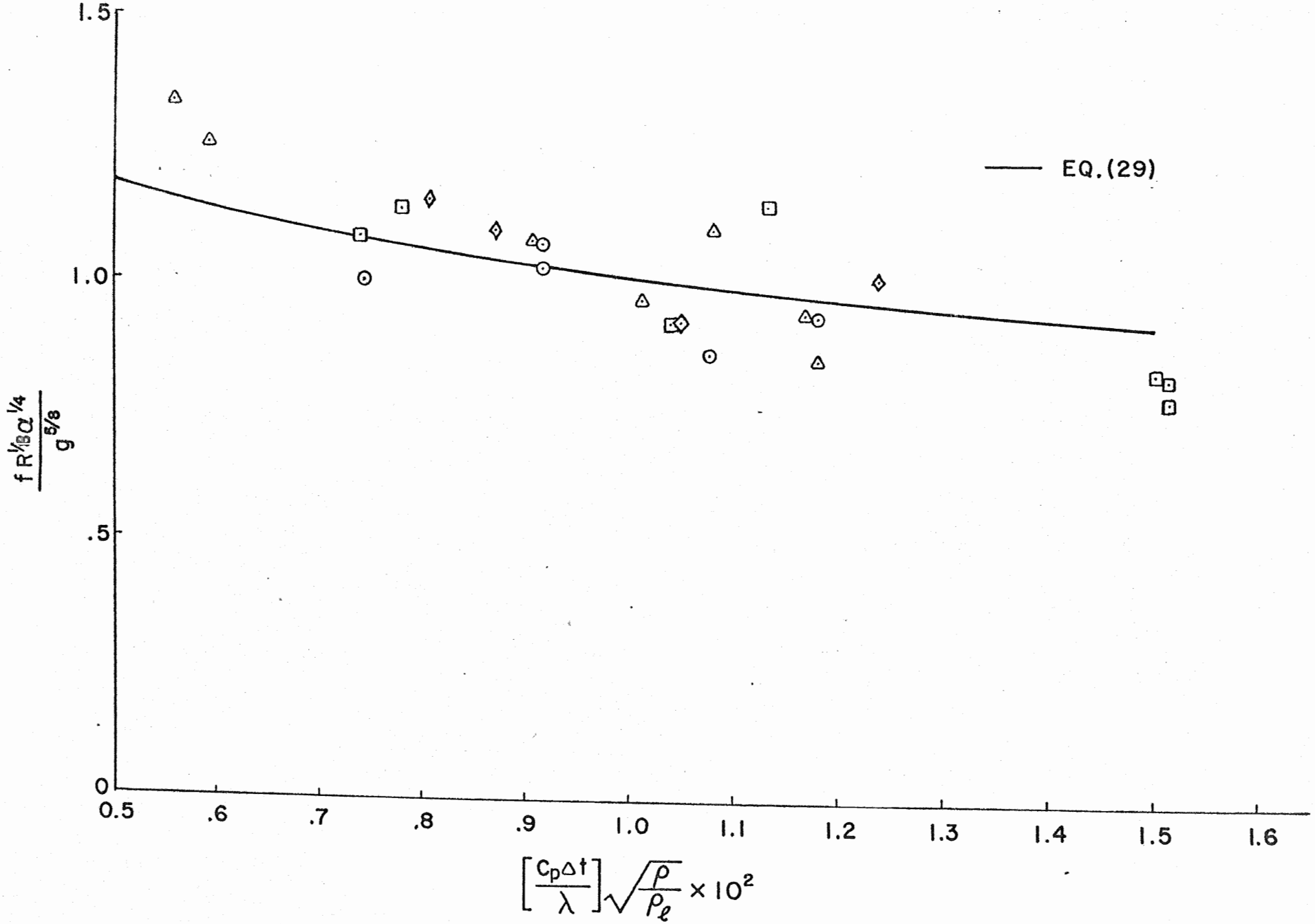
1.5
1.0
.5
0
0.5
.6
.7
.8
.9
1.0
1.1
1.2
1.3
1.4
1.5
1.6
EQ.(29)
$\frac{f R^{1/8} Q^{1/4}}{g^{5/8}}$
$\left[\frac{C_p \Delta t}{\lambda}\right]\sqrt{\frac{\rho}{\rho_\ell}} \times 10^2$

Figure 8.